

Optical transitions between valley split subbands in biased Si quantum wells

Michele Virgilio and Giuseppe Grosso

NEST-INFM and Dipartimento di Fisica "E. Fermi," Università di Pisa, Largo Pontecorvo 3, I-56127 Pisa, Italy

(Received 23 February 2007; revised manuscript received 9 May 2007; published 19 June 2007)

By a tight-binding $sp^3d^5s^*$ model, we study numerically the optical transitions involving the lowest conduction states confined in strained [001] Si quantum wells. These states belong to the fundamental and to the first excited quantum well (QW) subbands, each one split into a doublet by intervalley interaction. Both hard wall and finite SiGe barriers boundary conditions for the QWs are considered. Amplitudes of the doublet splittings as a function of the well width and of a uniform electric field superimposed along the growth direction are first investigated. Then, we study atomic contributions and parity character of the doublet wave functions to derive selection rules for interdoublet optical transitions. Finally, we demonstrate the role of intervalley coupling and the effectiveness of the selection rules here presented, for the interpretation of the absorption spectrum of a n -type Si QW between SiGe barriers, evaluated at different temperatures.

DOI: [10.1103/PhysRevB.75.235428](https://doi.org/10.1103/PhysRevB.75.235428)

PACS number(s): 78.67.De, 73.21.Fg, 73.61.Cw

I. INTRODUCTION

Bulk silicon has six degenerate energy minima (valleys) in the lowest conduction band along the $\langle 001 \rangle$ equivalent directions at 0.85 of the distance separating the Γ point from the X points at the centers of the square faces of the Brillouin zone. Breaking cubic symmetry, e.g., by means of uniaxial stress or other perturbations along the [001] axis, lifts the sixfold degeneracy into fourfold degenerate valleys in the plane orthogonal to the perturbing field and twofold degenerate valleys along the [001] direction.¹

As first evidenced by Fowler *et al.*² by means of magnetoconductance measurements in n -channel Si metal-oxide-semiconductor field-effect transistor inversion layers, also the twofold degeneracy can be lifted if the z valleys interact. This happens, for instance, when Si quantum wells are grown on a [001] substrate: heterointerfaces act as scatterers of the electronic waves and interference effects appear³ with phases depending on $2k_0z$, where \vec{k}_0 is the absolute minimum in \vec{k} space of the lowest Si conduction band. The vast theoretical and experimental literature on the subject up to the quantum Hall⁴ era at the beginning of the 1980s was exhaustively considered in the review.⁵

Recently, a renewed interest has been addressed toward the comprehension of the nature and the control of valley splitting in the context of nanostructures, in particular, for potential applications in the area of spintronics⁶ and spin-based quantum computation.^{7,8} In fact, beyond the bonuses derived from advances in crystal growth⁹ and processing technology, Si-based structures are expected to be particularly promising for their weak spin-orbit coupling and long electron spin decoherence time.¹⁰ This has strongly motivated the attempts of modulating the strength of intervalley coupling by means of external fields or specific system geometries. Even if a growing interest has been recently devoted to tilted or miscut heterointerface geometries,^{11–13} samples grown along the [001] direction remain the most studied due to their compatibility with the mainstream Si technology. Our work focuses on the optical transitions between valley split doublets in the conduction band of strained silicon quantum wells (QWs). We have established selection

rules based on the parity character of the doublet wave functions. Possible optical experiments able to detect valley coupling effects on the energy spectrum of Si QWs of different shapes are also presented.

Early theoretical descriptions of the origin of this valley splitting in Si exploited effective mass theory for single heterointerfaces¹⁴ and quantum wells¹⁵ and an sp^3s^* second neighbor tight-binding model¹⁶ for superlattices.

More recently, a detailed study of valley splitting of the lowest conduction band in Si quantum wells has been performed^{17,18} by means of a full band nearest neighbor $sp^3d^5s^*$ tight-binding model and a simple analytic two band model. The authors of Refs. 17 and 18 confirm previous results of Refs. 15 and 16, i.e., the lift of the twofold band degeneracy and an intervalley splitting which is different from zero also in the absence of electric fields. Moreover, they find sound numerical and model analytic support to the relation $\Delta E_0 \propto (S+2)^{-3} \sin[(S+2)\varphi_{min}]$ which describes the oscillations of the ground state doublet width as a function of the number S of atomic Si layers composing the quantum well; the phase φ_{min} is related to the position of the valley minimum \vec{k}_0 along the Δ line of bulk silicon.

A detailed analysis of effective mass formalisms and a comparison with atomistic tight-binding approaches for the evaluation of valley splitting in a heterostructure can be found in Refs. 3 and 12. The case of perfect or miscut Si QWs in the presence of external fields has also been studied,¹² showing that the insertion of an empirical contact potential to describe valley coupling in the effective mass method picks up the relevant physics of the problem.

In this paper, we present an $sp^3d^5s^*$ tight-binding study of the doublets generated by intervalley interaction in the fundamental and in first excited conduction subbands of a three dimensional strained [001] Si QWs. Our aim is to investigate the electronic properties and the optical transitions occurring between the fundamental and the first excited doublets as a function of the well width, the strength of an electric field applied along the \hat{z} axis, and temperature. Forbidden and allowed transitions are thus identified and dependence of optical selection rules on the field strength is discussed. Interpretation of the oscillator strengths for allowed transitions in

terms of the symmetries and shapes of the states in the well, both in the presence and in the absence of electric fields, is provided. Population effects on optical spectra induced by temperature are also analyzed.

We eventually show that valley splitting tuning by means of electric fields, temperature, and well width can be exploited to control conduction intersubband optical properties of Si QWs.

II. SYSTEM DESCRIPTION AND METHOD

We have considered a single Si quantum well grown along the [001] direction with tensile in-plane strain conditions compatible with growth on a relaxed $\text{Si}_{1-x}\text{Ge}_x$ substrate with Ge concentration $x_{sub}=0.2$. In the strained silicon region, the in-plane lattice constant, $a_{\parallel}(s-\text{Si})$, is matched to the relaxed substrate lattice constant, $a_0(x_{sub})$, which is evaluated (in angstrom units) according to Refs. 19 and 20,

$$\begin{aligned} a_{\parallel}(s-\text{Si}) &= a_0(x_{sub}) \\ &= a_0(\text{Si}) + 0.200\,326x_{sub}(1-x_{sub}) \\ &\quad + [a_0(\text{Ge}) - a_0(\text{Si})]x_{sub}^2, \end{aligned} \quad (1)$$

where $a_0(\text{Si})$ and $a_0(\text{Ge})$ are the lattice constants of relaxed silicon and germanium. The lattice constants along the growth direction are changed by the Poisson effect;^{21,22} in the well region, $a_{\perp}(s-\text{Si})$ is given by

$$a_{\perp}(s-\text{Si}) = a_0(\text{Si}) \left(1 - 2 \frac{c_{12}(\text{Si})}{c_{11}(\text{Si})} \frac{a_0(x_{sub}) - a_0(\text{Si})}{a_0(\text{Si})} \right). \quad (2)$$

Biaxial strain conditions guarantee lifting of the sixfold degeneracy of the lowest Si conduction band into a fourfold degenerate level corresponding to the four equivalent valleys in the (x,y) growth plane and a twofold degenerate level corresponding to the two equivalent valleys along the [001] direction. Tensile in-plane strain lowers²³ the energy of the twofold degenerate valleys with respect to the energy of the fourfold degenerate valleys. Intervalley interaction of these two minima further splits the twofold degeneracy into a doublet of nondegenerate levels.

For comparison with previous results, we have adopted the same QW system chosen in Refs. 17 and 18. Calculations have been performed both for a single strained silicon infinite QW (hard wall) and for a system composed by a strained Si finite QW embraced by two symmetric $\text{Si}_{0.4}\text{Ge}_{0.6}$ barriers. In the latter case, alignment of the topmost valence band between the tensile strained silicon and the compressive strained $\text{Si}_{0.4}\text{Ge}_{0.6}$ materials is performed according to the results of Refs. 24 and 25; the corresponding conduction band offset is ≈ 0.3 eV, which is a commonly accepted value.^{19,26} Barrier thickness is chosen so to ensure that the wave functions confined in the Si well are exhausted well before the system boundaries. Actually, for the above quoted value of the conduction band offset we have verified that the wave function amplitude in the barriers becomes negligible within a few atomic layers. Therefore, for the states confined in the well, we choose either periodic or nonperiodic boundary conditions along the growth axis. Anyway, if periodic

boundary conditions are not applied, a surface state band appears with energy minima below the energy of the ground state in the QW, thus preventing population of the QW ground state for very low doping concentrations. In the following treatment of optical properties and intervalley splitting, we disregard surface states.

For the self-energy and hopping energy parameters of the first-neighbor tight-binding $sp^3d^5s^*$ Hamiltonian, we have adopted the semiempirical parametrization of Jancu *et al.*²⁷ Biaxial strain was taken into account calculating the position of the ions in the strained lattice and scaling the hopping parameters with distances by means of suitable exponential laws as indicated in Ref. 27. The parameters for the SiGe alloys were obtained in the virtual crystal approximation.

The dimension of the crystal Hamiltonian is $N \times 10 \times 2$, where N is the total number of layers and 10×2 is the number of orbitals in the primitive cell in each layer; the factor 2 accounts for spin degeneracy. Each layer along the [001] direction contributes with a single atom; within the first-neighbor approximation, only adjacent layers interact. Typical order of the matrix Hamiltonians considered in this paper reaches 6×10^3 for the QW plus barrier systems. For the eigenvalues evaluation reported in the following, standard routines have been adopted. We have also investigated valley splittings for much larger systems ($N \sim 10^3$, not reported) for which the decimation-renormalization method²⁸ allows accurate indirect diagonalization of the Hamiltonian. In the latter case, the whole system Hamiltonian is represented on the basis of the two dimensional Bloch sums built from atomic orbitals.²⁹ Then, by iterative decimation-renormalization the matrix chain is reduced to a couple of effective layers where the Green's function is evaluated. From the poles of the Green's function, the spectral properties of the system are obtained without explicit diagonalization of the matrix Hamiltonian. From the Green's function also, layer and orbital resolved densities of states have been deduced. Further technical details on the method can be found in Ref. 30, where the same tight-binding model was adopted to interpret experimental valence intersubband spectra of SiGe heterostructures. The accuracy of the procedure allows us to safely resolve energy separations of the order of 10^{-5} – 10^{-6} eV, as evidenced by the evaluation of the doublet structure in the conduction band, and also from the numerical invariance of the layer and orbital densities of states under $x \leftrightarrow y$ transformations.

The evaluation of conduction intersubband transitions has been performed neglecting spin-orbit interaction in order to reduce computational time. In fact, we have checked that this assumption does not lead to appreciable effects in the valley splitting; spin-splitting correction to the conduction band states confined in silicon QW systems is relevant only at the μeV scale.³ Static electric fields along the growth direction are modeled superimposing to the system Hamiltonian an on site potential linearly varying along the \hat{z} axis.

Intersubband optical absorption for incident light with polarization unit vector $\hat{\epsilon}$ and energy $\hbar\omega$ incident on the QW system with refractive index n_0 (assumed independent of frequency in the energy range of interest) is given by³¹

$$\alpha(\hbar\omega) = \frac{2\pi e^2 \hbar}{n_0 c m_0 V \Gamma} \sum_{\vec{k}} \sum_{i,j} \frac{P_{ij}^\epsilon(\vec{k})}{E_i(\vec{k}) - E_j(\vec{k})} \cdot \{f[E_j(\vec{k})] - f[E_i(\vec{k})]\} \cdot \frac{1}{1 + \left(\frac{E_i - E_j - \hbar\omega}{\Gamma}\right)^2}, \quad (3)$$

where $P_{ij}^\epsilon(\vec{k}) = (2/m_0) |\langle i, \vec{k} | \hat{\epsilon} \cdot \vec{p} | j, \vec{k} \rangle|^2$ is the squared modulus of the dipole matrix element, expressed in eV, between conduction intersubband states $|j, \vec{k}\rangle$ and $|i, \vec{k}\rangle$ of energies E_j and E_i , respectively; $f(E)$ is the Fermi distribution function. Details on the calculation of the dipole matrix element in the tight-binding model can be found in Refs. 32–34. Line broadening effects are included in Eq. (3) by means of a Lorentzian distribution of linewidth $\Gamma = 1$ meV. Sums over \vec{k} are evaluated sampling a wedge of the Brillouin zone around the conduction minimum with up to 2.5×10^4 independent \vec{k} points.

III. RESULTS

A. Electronic structures

We have first studied the valley splitting magnitude of the QW lowest subband as a function of the well width. The oscillating behavior of the valley splitting and the power law decay of the oscillation envelope with the number of atomic layers composing the well have been reproduced (see Refs. 17 and 18). The small differences in the tight-binding parametrizations of Refs. 27 and 17 do not alter significantly the valley splitting results which are essentially governed by the position of the minimum \vec{k}_0 of the bulk Si conduction band. Then, we have analyzed the valley splitting doublet of the first excited subband, both for the infinite and the finite QWs.

In Fig. 1, we show the ΔE_0 (ΔE_1) splitting for the ground (first excited) doublet of the finite well as a function of the number of Si bilayers in the well and for different electric field strengths. Each bilayer is composed by two Si atomic layers in the anion and cation positions. For comparison, valley splittings for the hard wall QW at zero field are also reported. Damping of the oscillations with the well width of both the ΔE_0 and ΔE_1 doublets is evident. In Fig. 1, we can see that ΔE_0 and ΔE_1 oscillate with the same period and phase. This was expected extending to the ΔE_1 doublet the analytic considerations reported in Ref. 18 for the ΔE_0 doublet.

A superimposed electric field $\vec{\mathcal{E}}$ along the \hat{z} direction breaks the QW symmetry. Nevertheless, for low field strengths ($e\mathcal{E}W \lesssim E_0$ for the ground doublet and $e\mathcal{E}W \lesssim E_1$ for the first excited doublet, where W is the well width), the splitting oscillations persist with unchanged period and phase (see Fig. 1). Valley splitting becomes independent of the number of layers in the well only at high fields or large QW widths. This effect can be understood considering the E_0 and E_1 confinement energies and the spatial distributions of the wave functions within the QW: at zero or low electric field, E_0 and E_1 states have vanishing wave function at the barriers of the well; thus, valley splittings depend on the well width

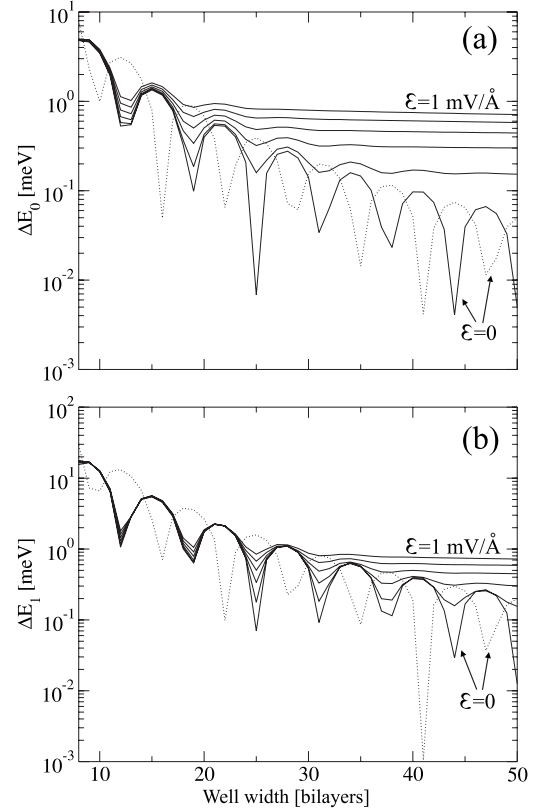


FIG. 1. Valley splitting magnitude versus well width for the ground [E_0 level, panel (a)] and first excited [E_1 level, panel (b)] QW subbands. Solid lines refer to the finite QW for electric field strengths ranging from 0 to 1 mV/Å. The dotted line represents the valley splitting for the hard wall system in the absence of electric field.

W (see the bottom inset of Fig. 2). For higher fields, the wave functions of the ground and of the first excited doublets become confined by the triangular shaped potential originated by the field and vanish before reaching the right interface of the QW (see the top inset of Fig. 2). In this case, the valley splitting is insensitive to the right interface position, i.e., to the well width. Moreover, in the limit of high electric fields the splittings of both the fundamental and excited doublets tend to a common value which is independent of the well width. This is evident in Fig. 2, where the ΔE_0 and ΔE_1 splittings are reported as a function of the field strength. The low field ($\mathcal{E} \lesssim 0.7$ mV/Å) flat behavior of ΔE_1 is due to the higher confinement energy of the excited E_1 doublet which makes it less sensitive to the profile of the bottom of the QW.

For what concerns the wave functions of the doublets, as previously found^{16,17} we obtain that they can be described as product of a square well envelope function and a fast oscillating function whose period (about five atomic monolayers) is governed by the Si conduction band minima. A discussion on point symmetry in SiGe structures can be found in Refs. 3 and 35. In the system we have studied, due to intervalley interaction, the states of the symmetric Si QW are nondegenerate and thus have well defined parity. The states within the same doublet share the same envelope function; therefore, they must have opposite parities to preserve orthogonality.

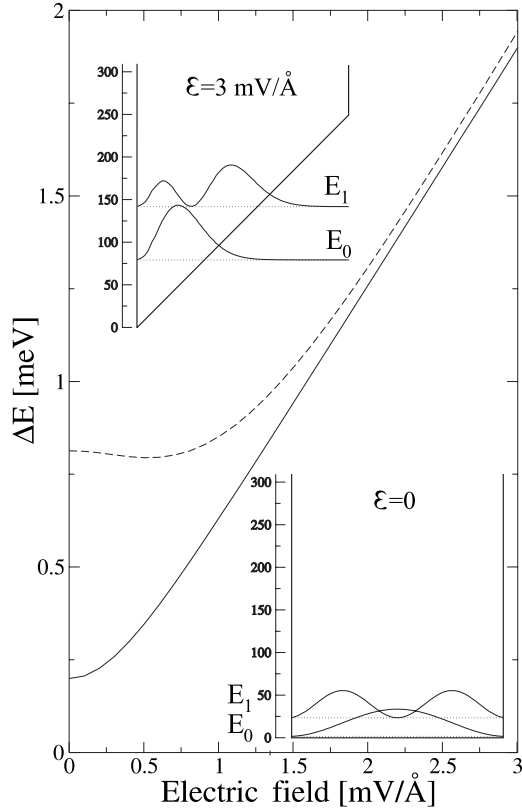


FIG. 2. Valley splitting magnitude for the ground (ΔE_0 , solid line) and first excited (ΔE_1 , dashed line) doublets versus electric field strength. The results refer to an infinite quantum well composed of 31 Si bilayers, corresponding to a maximum in the oscillation of the valley splitting amplitude (see Fig. 1, dotted line). The insets report the average value of the ground and first excited doublet energies, with squared modulus of the corresponding wave functions in the absence (bottom) and in the presence (top) of an electric field of strength of 3 mV/Å. Similar results hold for the finite well system.

Consequently, the phase of the wave function oscillations has to agree with the even or odd character of the state. From inspection of the orbital resolution of the wave functions numerically obtained with our model, we find that the E_0 and E_1 states have nonzero contributions only from the set of orbitals s , s^* , d_{xy} , $d_{3z^2-r^2}$ (even under $z \rightarrow -z$ transformation) and from the p_z orbitals (odd). Because the envelope function of the E_0 doublet is even, the oscillating modulation for the s , s^* , d_{xy} , $d_{3z^2-r^2}$ contributions to the wave function of the $E_0^{(1)}$ even ($E_0^{(2)}$ odd) states has to be cosine- (sine-) like, while it has to be sine- (cosine-) like for the p_z orbital contribution. Since the envelope function of the first excited doublet E_1 is odd, the opposite holds for the states of the corresponding excited doublet.

The above considerations are confirmed by our numerical results for the wave function amplitude of the states confined in the finite and infinite wells. For instance, for the case of a 128 monolayer width infinite well, we report in Figs. 3(a) and 3(c) the wave function amplitude, at field $\mathcal{E}=0$, of the lower level $E_0^{(1)}$ belonging to the E_0 doublet. $E_0^{(1)}$ results to be even and Fig. 3(a) [Fig. 3(c)] shows the total contribution to

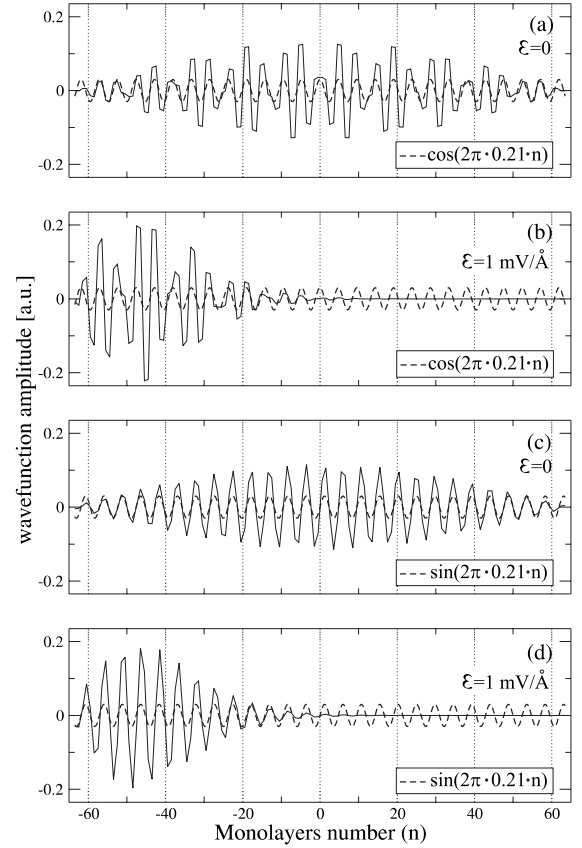


FIG. 3. Wave function amplitude of the even $E_0^{(1)}$ state for the infinite quantum well with thickness of 128 monatomic layers. Plots (a) and (b) refer to the even orbital contribution (s , s^* , d_{xy} , and $d_{3z^2-r^2}$) at $\mathcal{E}=0$ and $\mathcal{E}=1$ mV/Å, respectively. Plots (c) and (d) refer to the odd orbital contribution (p_z) at $\mathcal{E}=0$ and $\mathcal{E}=1$ mV/Å, respectively. Cosine and sine functions with analytic expressions indicated in the insets are superimposed to the wave functions of $E_0^{(1)}$ to evidence phases and period of the oscillations as discussed in the text. The center of the well is set at $z=0$. Similar results hold for the $E_0^{(2)}$, $E_1^{(1)}$, and $E_1^{(2)}$ levels.

the oscillating modulation of the wave functions from the even (odd) orbitals. To evidence phase and period of the wave function oscillations, we have superimposed in Figs. 3(a)–3(d) even and odd harmonic functions as indicated in the corresponding insets. We also find that period and phase of the oscillations are unaffected by the presence of an electric field [see Figs. 3(b) and 3(d)] even if it breaks the QW symmetry and modifies the wave function envelope.

B. Optical properties

Let us now consider the optical transitions between the levels of the ground doublet $E_0^{(1)}$, $E_0^{(2)}$ and the levels of the first excited doublet $E_1^{(1)}$, $E_1^{(2)}$. Since low doping concentrations are needed to resolve the doublet structure, we will focus on transitions occurring in a small neighbor of the bottom of the conduction band. Intersubband transitions between the fundamental and first excited subband are induced only by light incident parallel to the growth plane,³⁶ thus the polarization vector $\hat{\epsilon}$ in Eq. (3) is chosen along the \hat{z} axis.

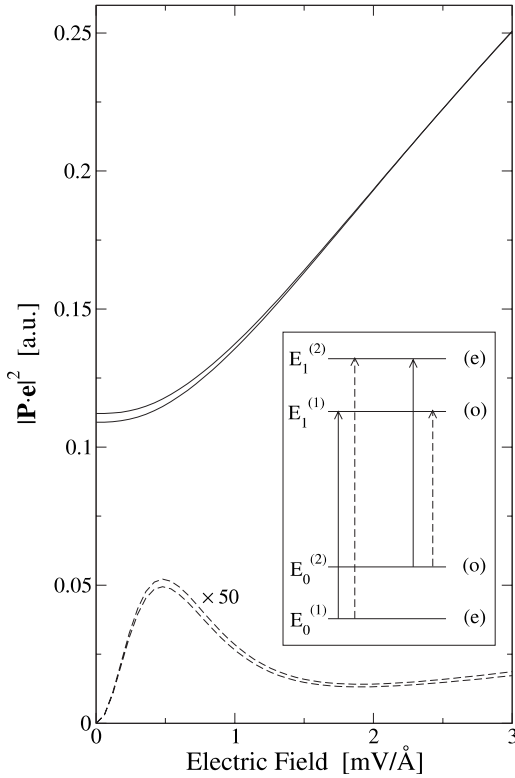


FIG. 4. Dipole matrix elements for intersubband transitions between the doublet $(E_0^{(1)}, E_0^{(2)})$ and the doublet $(E_1^{(1)}, E_1^{(2)})$ as function of the electric field. A 31 bilayer thick silicon infinite quantum well is considered. The results refer to the bottom of the conduction band and polarization vector \hat{e} along the \hat{z} axis. Solid (dashed) lines indicate transitions between states with equal (opposite) parity for $\mathcal{E} = 0$. In the inset, even (e) and odd (o) parities of the states at zero field and forbidden and allowed transitions at zero field are sketched. For allowed transitions, the dipole matrix element increases with the field due to the confinement of the states in narrower spatial regions.

As also reported in Refs. 3, 17, and 37, we find numerically that the parity of the ground state is an alternating function of the well width. As already noticed, within each doublet the states have opposite parities. Since for incident light polarized along the \hat{z} axis the dipole operator is odd for reflection in the xy plane, at zero field light couples only states with opposite parities (see the inset of Fig. 4). Numerical calculations of the dipole oscillation strength at the bottom of the conduction band for the $(E_0^{(1)}, E_0^{(2)}) \rightarrow (E_1^{(1)}, E_1^{(2)})$ transitions confirm this statement: we find that at zero field the parity selection rules are respected with great precision.

To observe transitions between states with the same parity, it is necessary to break the $z \rightarrow -z$ symmetry. For this reason, we have investigated the oscillation strength of these transitions when an electric field along the growth direction is superimposed (see Fig. 4). Our results indicate that even for strong electric fields no appreciable oscillation strength is transferred to the transitions which are forbidden at zero field; in fact, they remain much weaker than the allowed ones. This is rather surprising if one considers that at $\mathcal{E} \approx 3$ mV/Å the wave functions are confined in the left por-

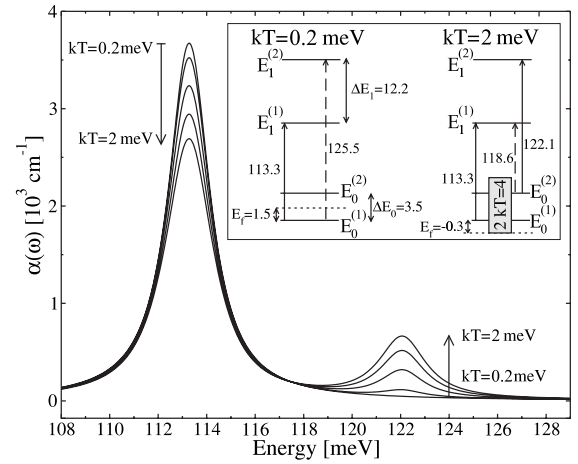


FIG. 5. Intersubband absorption spectra for a silicon finite QW with $\text{Si}_{0.4}\text{Ge}_{0.6}$ barriers. Well width is 10 bilayers and the carrier concentration in the well region is $7.5 \times 10^{-7} \text{ \AA}^2$ per layer. kT ranges from 0.2 to 2 meV. Energy separations for the E_0 and E_1 doublets and Fermi energies calculated at $kT=0.2$ meV and $kT=2$ meV are summarized in the inset (not to scale). Solid and dashed arrows refer to allowed and forbidden transitions, respectively. Energies are expressed in meV.

tion of the well by the triangular potential generated by the field [also see Figs. 3(b) and 3(d)].

We now show that the above selection rules obtained numerically can be verified by absorption measurements. In fact, at low fields the valley splitting magnitudes of the E_0 and E_1 doublets are not equal (see Fig. 2). Therefore, the allowed $(E_0^{(1)} \rightarrow E_1^{(1)}, E_0^{(2)} \rightarrow E_1^{(2)})$ and the forbidden $(E_0^{(1)} \rightarrow E_1^{(2)}, E_0^{(2)} \rightarrow E_1^{(1)})$ transitions may occur at quite different energies. For instance, as can be argued in Fig. 1, for QW systems with well width of ≈ 10 bilayers, the transition energy differences are of the order of a few meV and then the related absorption peaks can be experimentally resolved.

A possible experiment is suggested by the results of Fig. 5 where we have reported the intersubband optical spectra of a 10 bilayer finite QW at different temperatures. At chosen doping concentration, subband population can be selectively controlled by thermal energy and thus the signature of allowed and forbidden transitions can be monitored. Let us consider in fact, the inset of Fig. 5. It refers to a carrier concentration in the well region of $7.5 \times 10^{-7} \text{ \AA}^2$ per layer. At low temperatures ($kT \leq 0.2$ meV), the Fermi energy lies below the $E_0^{(2)}$ level and carriers are not thermally excited in this state. Therefore, one single absorption peak due to the $E_0^{(1)} \rightarrow E_1^{(1)}$ transition (113 meV) is expected in the optical spectrum, the $E_0^{(1)} \rightarrow E_1^{(2)}$ (125.5 meV) transition being forbidden. Increasing the temperature, the Fermi energy decreases but now carriers can be thermally promoted in the $E_0^{(2)}$ level; at $kT=2$ meV, we find $E_f = -0.3$ meV and because the ΔE_0 separation is 3.5 meV, we have $E_0^{(2)} - E_0^{(1)} < 2kT$ (see inset). Then, also the $E_0^{(2)} \rightarrow E_1^{(2)}$ transition (122.1 meV) should give a peak in the spectrum, while no signal for the forbidden $E_0^{(2)} \rightarrow E_1^{(1)}$ transition (118.6) is expected. The intersubband absorption spectra evaluated at finite temperatures, sampling the QW \vec{k} space around the conduction mini-

num and reported in Fig. 5, support the above considerations. At $T \lesssim 0.2$ meV, only the $E_0^{(1)} \rightarrow E_1^{(1)}$ signal is present; increasing T , oscillator strength is transferred from the $E_0^{(1)} \rightarrow E_1^{(1)}$ to the $E_0^{(2)} \rightarrow E_1^{(2)}$ transition. No absorption for the forbidden transitions (125.5 and 118.6 meV) is found in the explored range of temperatures.

IV. CONCLUSIONS

We have adopted a tight-binding Hamiltonian to investigate the valley splitting of confined subbands in strained infinite Si QW systems and in strained Si/SiGe QW systems with finite height barriers. The splittings are due to the interaction between the two conduction valley minima along the growth direction of the silicon crystal. We have studied the energy separation of the fundamental and first excited doublets as a function of the well width both for symmetric QWs

and for QWs with uniform electric field superimposed along the growth direction. Results for the wave functions of the confined states have been reported and their symmetry properties in the presence and in the absence of an electric field discussed in detail. We have then studied the optical transitions between states of the fundamental and of the first excited doublets. Guided by symmetry arguments and numerical calculations, we have predicted selection rules for these transitions. Finally, the evaluated intersubband absorption spectrum here presented for a realistic n -type Si/SiGe QW system at different temperatures suggests possible absorption measurements involving transitions between valley split Si levels.

ACKNOWLEDGMENT

This work has been supported by National Enterprise for NanoScience and NanoTechnology (NEST).

-
- ¹F. Stern and W. E. Howard, Phys. Rev. **163**, 816 (1969).
²A. B. Fowler, F. F. Fang, W. E. Howard, and P. J. Stiles, Phys. Rev. Lett. **16**, 901 (1966).
³M. O. Nestoklon, L. E. Golub, and E. L. Ivchenko, Phys. Rev. B **73**, 235334 (2006).
⁴K. v. Klitzing, G. Dorda, and M. Pepper, Phys. Rev. Lett. **45**, 494 (1980).
⁵T. Ando, A. B. Fowler, and F. Stern, Rev. Mod. Phys. **54**, 437 (1982).
⁶S. A. Wolf, D. D. Awschalom, R. A. Buhrman, J. M. Daughton, S. von Molnár, M. L. Roukes, A. Y. Chtchelkanova, and D. M. Teger, Science **294**, 1488 (2001).
⁷D. Loss and D. P. DiVincenzo, Phys. Rev. A **57**, 120 (1998).
⁸B. E. Kane, Nature (London) **393**, 133 (1998).
⁹K. Brunner, Rep. Prog. Phys. **65**, 27 (2002).
¹⁰A. M. Tyryshkin, S. A. Lyon, W. Jantsch, and F. Schäffler, Phys. Rev. Lett. **94**, 126802 (2005).
¹¹M. Friesen, M. A. Eriksson, and S. N. Coppersmith, Appl. Phys. Lett. **89**, 202106 (2006).
¹²M. Friesen, S. Chutia, C. Tahan, and S. N. Coppersmith, Phys. Rev. B **75**, 115318 (2007).
¹³S. Lee and P. von Allmen, Phys. Rev. B **74**, 245302 (2006).
¹⁴L. J. Sham and M. Nakayama, Phys. Rev. B **20**, 734 (1979).
¹⁵F. J. Ohkawa, Solid State Commun. **26**, 69 (1978).
¹⁶G. Grosso, G. Pastori Parravicini, and C. Piermarocchi, Phys. Rev. B **54**, 16393 (1996).
¹⁷T. B. Boykin, G. Klimeck, M. A. Eriksson, M. Friesen, S. N. Coppersmith, P. von Allmen, F. Oyafuso, and S. Lee, Appl. Phys. Lett. **84**, 115 (2004).
¹⁸T. B. Boykin, G. Klimeck, M. Friesen, S. N. Coppersmith, P. von Allmen, F. Oyafuso, and S. Lee, Phys. Rev. B **70**, 165325 (2004).
¹⁹M. M. Rieger and P. Vogl, Phys. Rev. B **48**, 14276 (1993).
²⁰J. P. Dismukes, L. Ekstrom, and R. J. Paff, J. Phys. Chem. **68**, 3021 (1964).
²¹See, e.g., J. Singh, *Electronic and Optoelectronic Properties of Semiconductor Structures* (Cambridge University Press, Cambridge, 2003).
²²C. G. Van de Walle and R. M. Martin, Phys. Rev. B **34**, 5621 (1986).
²³D. J. Paul, Semicond. Sci. Technol. **19**, R75 (2004).
²⁴M. Virgilio and G. Grosso, J. Phys.: Condens. Matter **18**, 1021 (2006).
²⁵L. Colombo, R. Resta, and S. Baroni, Phys. Rev. B **44**, 5572 (1991).
²⁶F. Schäffler, Semicond. Sci. Technol. **12**, 1515 (1997).
²⁷J.-M. Jancu, R. Scholz, F. Beltram, and F. Bassani, Phys. Rev. B **57**, 6493 (1998).
²⁸G. Grosso and G. Pastori Parravicini, *Solid State Physics* (Academic, London, 2000).
²⁹G. Grosso, S. Moroni, and G. P. Parravicini, Phys. Rev. B **40**, 12328 (1989).
³⁰M. Virgilio and G. Grosso, J. Appl. Phys. **100**, 093506 (2006).
³¹*Intersubband Transitions in Quantum Wells*, edited by E. Rosencher, B. Vinter, and B. F. Levine (Plenum, New York, 1992).
³²S. Y. Ren and W. A. Harrison, Phys. Rev. B **23**, 762 (1981).
³³L. Brey and C. Tejedor, Solid State Commun. **48**, 403 (1983).
³⁴F. Trani, G. Cantele, D. Ninno, and G. Iadonisi, Phys. Rev. B **72**, 075423 (2005).
³⁵L. E. Golub and E. L. Ivchenko, Phys. Rev. B **69**, 115333 (2004).
³⁶M. Virgilio and G. Grosso, Nanotechnology **18**, 075402 (2007).
³⁷J.-C. Chiang, Jpn. J. Appl. Phys., Part 2 **33**, L294 (1994).